Petroleum and Coal

Article **Open Access**

Evaluation of Production Potential of Fractured Geothermal Systems Due to Cold Fluid Circulation under Poro-Thermo Elastic Conditions

Reda Abdel Azim

American University of Ras Al Khaimah, United Arab of Emirates, Ras Al Khaimah

Received August 19, 2017; Accepted December 1, 2017

Abstract

In this study, the fractured geothermal reservoir behavior due to injection and circulation of cold fluid is evaluated under a poro-thermo-elastic environment by taking into consideration the dilation of fracture surface. 3D reservoir simulator is generated in house using finite element method and coupled poro-thermo-elastic approach. The proposed approach is applied on a selected volume of Soultz reservoir to assess the permeability enhancement over stimulation period of more than 3 month and fluid circulation period of 14 years. The results show that the fracture permeability (aperture) does not change in the first three weeks of cold fluid injection and it takes longer period to reach a certain level of growth in average fracture aperture. In addition, it was observed that thermal stresses have a substantial impact on the distribution of the three component of reservoir effective stresses in x-.y-, and z- directions, the produced fluid temperature and fracture permeability as well. In addition, thermal stresses have a notable contribution in increasing the fracture aperture which in turn increases the injectivity of the well and leads to creation of flow channeling between the injection and production wells.

Keywords: *Naturally fractured reservoir; Geothermal.*

1. Introduction

The geothermal energy is defined as the energy stored in the form of heat in the earth's crust or in the reservoirs located in deep. The source of heat origination is created from: (1) radiogenic heat due to the decay of natural radioactive materials; (2) heat generated during the earth formation and the energy released during the formation process ;(3) frictional heat resulting from earthquake [1]. The temperature increases from the surface to the center of the earth's crust on the average value of 3°C per 100 m. The majority of the earth crust temperature is hotter than 1000°C, so it provides a comprehensive heat potential which it can be used in many projects, places and various applications.

Hot dry geothermal reservoir is considered one main potential sources of renewable energy to produce a huge amount of electrical power. The heat can be recovered by injecting the cold water from the surface into the fractured reservoir through injectors and then to the surface passing through turbines to produce electricity, and by injection the fluid back into the heat-depleted rock to close the loop. This method called Enhanced Geothermal System [2] (EGS). In order to achieve the highest efficiency from the HDR system, the rock temperature should not be less than 200°C and the temperature of the produced fluid at the well head (producer) should be more than 180°C.

Simulation of thermal, hydrological, mechanical and chemical (THMC) process in naturally fractured geothermal reservoir is introduced for many years ago. The simulation of these processes is performed at very simple numerical methods with many assumptions used. The introducing of the analytical techniques with completely uncoupled approach was stronger than the numerical methods at that time. After the development of the numerical methods,

the finite element approach has been introduced as strong tool used in simulation of THMC process in naturally fractured geothermal reservoirs.

During the process of production, the circulated fluid inhibits the pressure solution process, mineral precipitation, and thermo mechanical aperture closure. The pressure solution phenomena, which is the most common in sandstone and extremely low in metamorphic rock, takes place with the transform of one particle into another, and with the truncation of fossils, thus leads to deformation of rocks [3].

Yashura *et al.*, [4] proposed a mechanistic model which describes the closure of fracture and aperture change is a result of the pressure solution, permeability reduction and mineral precipitation at the fracture face as a result of deviatoric stress. The model showed that the rate of aperture reduction increases as temperature and effective stress increase. Although the model assumed that the relationship between stress and the reduction of aperture is a linear function, as example, doubling the stress roughly doubles the closure rate, and this is a weak point, but also it considered one of the pioneers model dealt with the coupling process.

In 1990, a first numerical model has been appeared by [5-6], they developed finite-difference model coupled with analytical techniques used to assess the altering in fracture aperture with time and also fluid pressure during precipitation of quartz. The study assumed that a single fracture exist within the reservoir and located between two impermeable layers of granitic rock. As the water injected through the fractured, the rocks will cool, leading to thermal stresses and mineral precipitations.

Toran *et al.*, [7] introduced a new methodology and numerical simulator for the modeling of coupling process (thermal-hydrological-mechanical-chemical) process in naturally fractured geothermal reservoir. They used the model to evaluate the alterations of permeability and porosity value due to as dilation of fracture aperture as a result of the thermal stress effects. The results have been shown that, the influence of mechanical behavior started one month after the beginning of the injection process. In addition, the chemical effect influence on the permeability and porosity values started to act after 1 year of cold water injection especially near to the injection well.

Koh *et al.*, [8] research stated that in situ stress has a significant impact on fluid flow and amount of heat transfer between the fluid and the rock. This effect will change the rock properties as permeability and porosity values. A thermo –poro-elastic modeling is coupled with fracture geo-mechanical model and presented in this paper in order to understand the response of fracture systems with changing in effective stresses, specially the long term of geo-mechanical effects of thermal stresses on the reservoir properties. The main contribution of this paper is that this model can evaluate the changes in permeability and porosity with time with a stochastic distribution of the fractures in the reservoir, and overwhelmed the assumptions that have been presented by Ghassemi and Kumar [9]. The model is applied to naturally fractured reservoir with a fracture density 0.25 m-1, and the distance between the injector- producers well is 565 meter. Parameters of pressure loss, flow rate, temperature of produced water, temperature drawdown, and thermal stresses were calculated within a production period of 10 years. Results had shown that, a tensile thermal stress force created when the temperature of the geothermal reservoir started to drop due to the shrinkage of the rock [10]. This will lead a creation of cracks in the existing fractures [11], hence; the permeability will increase. The majority effect of the thermal stress is near to the injection well, and this observed for short term effect< 1 year. The chemical effect has not been coupled during the model running.

Shaik *et al.*, [12] they investigated the role of heat transfer between fluid and rock to evaluate the producing reservoir from the economical side by formulating a numerical model with two wells (producer and injector). This proposed approach links between all fractures properties (aperture, length and orientation) in simulating fluid flow and their effect on heat capture by the injected fluid. Low to – medium density fractures case is assumed during the evaluation of hot water production potential in the constructed numerical model. Many scenarios have been performed with the numerical model of different injection scenarios in order to determine

the thermal drawdown for a given reservoir. The results of this study have been indicated that the optimizing of the producing geothermal reservoir is extremely urgent issue, as for example, there is a threshold flow rate from the injector to the producer, above this threshold value the reservoir will subject to a rapid cooling effect. This threshold value strongly depends on the fracture density and the heat transfer between a rock and fluid. The high pressure loss is also encountered between the injector and producer for both cases of low – to medium fractures. Any increasing encountered in heat –transfer coefficient for a given geothermal reservoir, will increase the opportunity for the injected fluid to capture the maximum amount of heat from the rock. Finally, every geothermal reservoir has its own optimum flow to extract large volume of heat. The limitation of this paper is consider the thermal conductivity of rock constant with time.

In this paper, we present a fully coupled poro-thermo elastic model to simulate and assess the production potential of Soultz geothermal reservoir. The model is based on a hybrid approach (single continuum and discrete fracture approach) to calculate the permeability alteration due to cold water injection. The thermo-poro elastic framework that used in the simulation process has been derived by using mass, energy, and momentum balance equations.

2. Model setup

A case study is carried out to assess the response of Soultz geothermal reservoir due to fluid injection during stimulation and its production potential due to circulation of cold water under thermo poroelastic effect. The derivation of thermo poroelastic equations is presented.

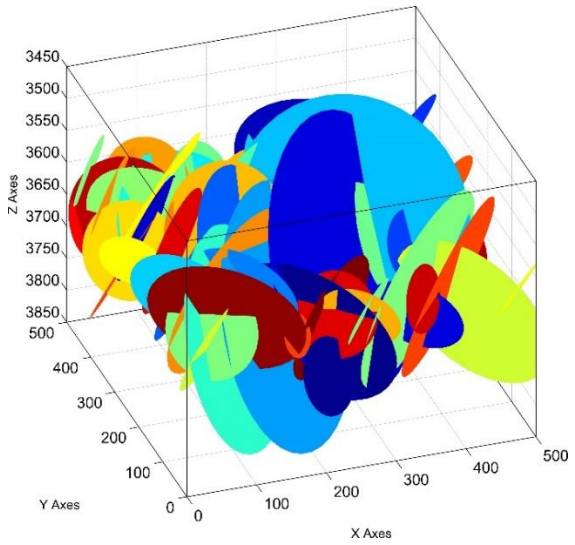

Fig.1. A schematic representation of the discrete fracture network of the selected volume of Soultz geothermal reservoir. *After* [14]

The reservoir dimensions are 500m× 500m×100m along x-, y- and z- directions respectively. The depth from the top of the reservoir is 3600m. Two wells, one is placed at the left corner of the domain as injector and the other one placed at the right corner as producer. 3D meh is generated (for fractured network in Fig.1) using 62,453 tetrahedral elements. 3D permeability tensors are calculated for small to medium fractures of length (l<60m) and long fracture are discretized explicitly in the domain.

The reservoir is initialized by values of rock and fluid properties and stress boundary conditions along the x-, y- and z- directions respectively. The data used in this study are presented in Table 1. The reservoir response is tested first by injecting high fluid pressure (42.5MPa) and the change in discrete fracture aperture is monitored with time. In this paper, the aperture change due to injected fluid pressure is calculated using Willis- Richard *et al.* [13] method. In this method, the change in fracture is caused by shear slippage. The shear slippage is controlled by the concept of shear failure using linear Mohr-Coulomb criterion in which, the shear slippage occurs when the shear stress exceeds rock shear strength.

Initially, when the fracture surfaces are in contact, the fracture aperture (a) is given by [13] as follow (see Fig.2):

$$a = \frac{a_0}{1+9^{\sigma_{eff}/\sigma_{nref}}} + a_s + a_{res} \qquad (1)$$

where: a_0 is the initial fracture aperture, a_s is the increase in fracture aperture due to shear dilation, a_{res} is the residual aperture at high effective stress and considered to be zero in this paper, and σ_{nref} is the effective normal stress.

Table 1. Stress and rock input data for the Soultz geothermal reservoir [8,15]

Parameter	Value	Parameter	Value
Young's modulus (GPa)	40	Fluid density (Kg/m^3)	1000
Poisson's ratio	0.2	Injector pressure, stimulation (MPa)	42.5 (6163psi)
Density (Kg/m^3)	2700	Injector pressure, circulation (MPa)	37.5 (5439pai)
Shear dilation angle (deg)	3	producer pressure, circulation (MPa)	31.5 (4569psi)
Matrix permeability (m^2)	5.2×10^{-17}	Wellbore radius (m)	0.1
Fracture shear stiffness (Pa/m)	1.37×10^{9}	Reservoir depth (m)	3600-3700
Fracture basic friction angle (deg)	34	Specific heat (rock) (Jkg^{-1}K^{-1})	1.098×10^{3}
Largest fracture radius (m)	197.3	Specific heat (fluid) (Jkg^{-1}K^{-1})	4.05×10^{3}
Smallest fracture radius (m)	9.5	Thermal Conductivity (rock) (Wm^{-1}s^{-1})	2.58
Vertical stress (MPa)	91.78 (13311psi)	Thermal Conductivity (fluid) (Wm^{-1}s^{-1})	0.68
Maximum horizontal stress (MPa)	91.06 (13206psi)	Initial reservoir pressure(MPa)	34.5
Minimum horizontal stress (MPa)	49.54 (7185psi)	Initial reservoir temperature (°C)	200
90% Closure stress (MPa)	30	Injecting Fluid Temperature(°C)	80
Fluid viscosity (Pa s)	3×10^{-4}		

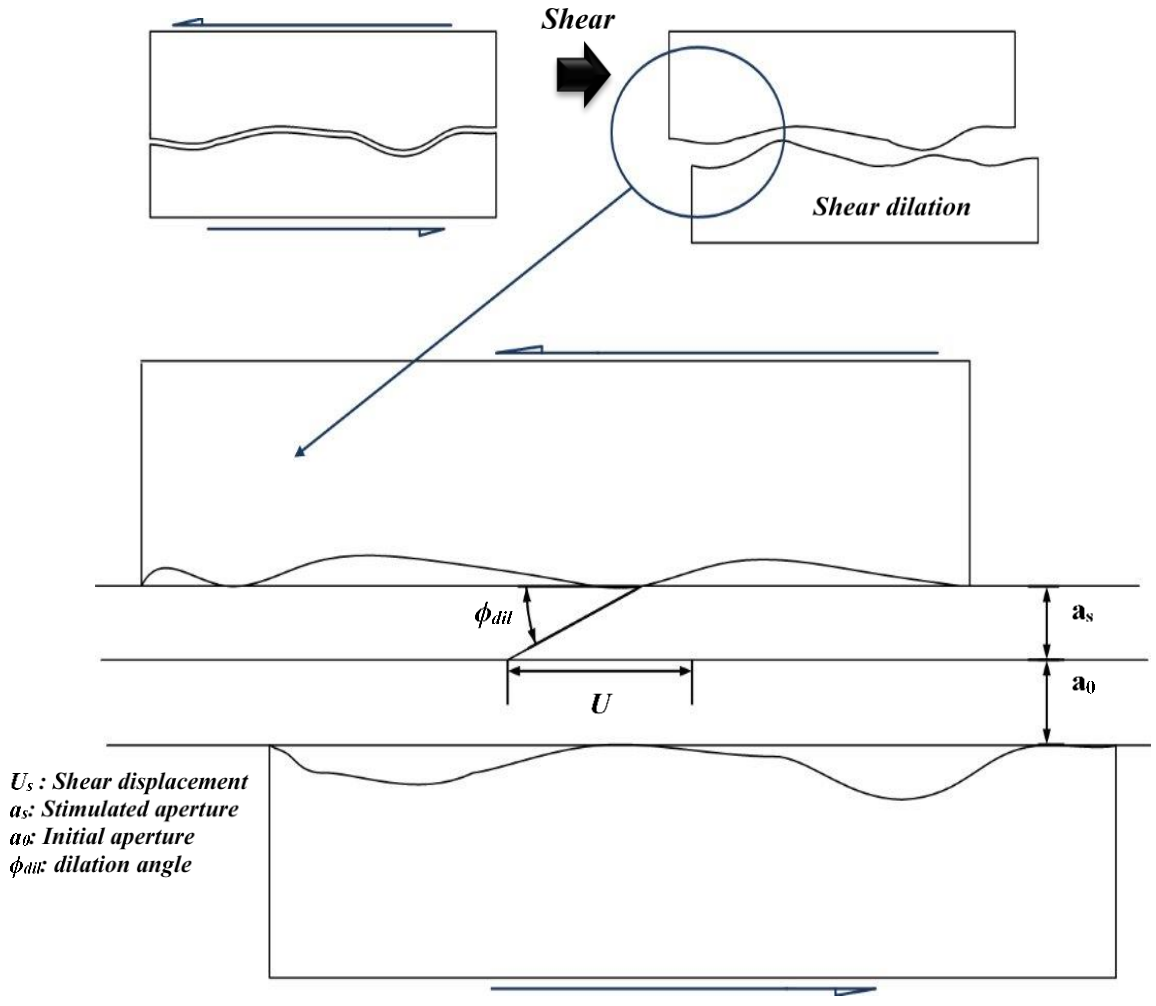

Fig. 2. Calculation of change in aperture due to cold water injection using Willis- Richard *et al.* method [13]

When the pressure inside the fracture becomes higher than the effective normal applied stress, the fracture surfaces is no longer in contact and starts to open. The shear displacement in this condition can be expressed as:

$$U_s = \frac{\tau_n}{K_s} \quad (2)$$

where τ_n the shear is stress and K_s is the fracture shear stiffness. The change in fracture aperture (a_s) due to shear dilation can be expressed as:

$$a_s = U_s \tan(\varphi_{dil}^{eff}) \quad (3)$$

where φ_{dil}^{eff} is the effective shear dilation angle. The total aperture after the shear can be calculated as:

$$a = \frac{a_0}{1+9^{\sigma_{eff}/\sigma_{nref}}} + U_s \tan(\varphi_{dil}^{eff}) \quad (4)$$

2.1. Derivation of Governing Equation for Thermo poroelastic model

The equations used to simulate thermo-poroelastic coupling process are momentum, mass and energy conservation. These equations are presented in details in this section.

Momentum Conservation

The linear momentum balance equation in terms of total stresses for can be written as:

$$\nabla \cdot \sigma + \rho g = 0 \quad (5)$$

where, σ is the total stress, g is the gravity constant and ρ is the bulk intensity of the porous media. The intensity should be written for two phases, liquid and solid as follows:

$$\rho = \varphi\rho_l + (1-\varphi)\rho_s \quad (6)$$

Equation (E.1) can be written in terms of effective stress as follows:

$$\nabla \cdot (\sigma' - pI) + \rho g = 0 \quad (7)$$

where, σ is the effective stress, p is the pore pressure, and I is the identity matrix. This equation for the stress-strain relationship does not contain thermal effects and to include the thermo elasticity, the equation can be written as follow:

$$\sigma' = C(\varepsilon - \alpha_T \Delta T \times I) \quad (8)$$

where, C is the fourth-order stiffness tensor of material properties, ε is the total strain, α_T is the thermal expansion coefficient and ΔT is the temperature difference. The isotropic elasticity tensor C is defined as:

$$C = \lambda\delta_{ij}\delta_{kl} + 2G\delta_{ik}\delta_{jl} \quad (9)$$

where, δ is the Kronecker delta, λ is the Lame constant. G is the shear modulus of elasticity.

The constitutive equation for the total strain-displacement relationship is defined as follows:

$$\varepsilon = \frac{1}{2}\left(\nabla\vec{u} + \left(\nabla\vec{u}\right)^T\right) \quad (10)$$

where, $\vec{u}$ is the displacement vector and ∇ is the gradient operator.

Mass Conservation

The fluid flow in deformable and saturated porous media can be described by the following equation:

$$S_s \frac{\partial p}{\partial t} + \beta \nabla . \left(\frac{\partial \vec{u}}{\partial t} \right) + \nabla . q - \alpha_T \frac{\partial T}{\partial t} = Q \qquad (11)$$

where, β is the Biots coefficient and assumed to be =1.0 in this study, p is the pore fluid pressure, T is the temperature, α_T is the thermal expansion coefficient, q is the fluid flux, and Q is the sink/source and S_s is the specific storage which is defined by the following Eq. (12).

$$S_s = (\frac{1-\varphi}{K_s}) + (\frac{\varphi}{K_l}) \qquad (12)$$

where, K_s is the compressibility of solid and K_l is the compressibility of liquid.

The fluid flux term (q) in the mass balance in **Eq. (E.11)** can be described by using Darcy's flow equation because of the intensity has been assumed constant in this study:

$$q = -\frac{k}{\mu}(\nabla p - \rho \vec{g}) \qquad (13)$$

where, k is the permeability of the domain. The Cubic law is used in determining fracture permeability.

Energy Conservation

The energy balance equation for heat transport through porous media can be described as follow:

$$(\rho c_p)_{eff} \frac{\partial T}{\partial t} + \nabla . q_T = Q_T \qquad (14)$$

where, q_T is the heat flux, Q^T is the heat sink/source term, and ρc_p is the heat storage and equals to;

$$(\rho c_p)_{eff} = \varphi (c_p \rho)_{liquid} + (1-\varphi)(c_p \rho)_{solid} \qquad (15)$$

In this study, conduction and convection heat transfers are considered during numerical simulation. The heat flux term in Eq. (14) can be written as:

$$q_T = -\lambda_{eff} \nabla T + (c_p \rho)_{liquid} v \cdot T \qquad (16)$$

where, *v* is the velocity of the fluid.

The first term on the right hand side of Eq. (15) is the conduction term and the second term is the convective heat transfer term and λ_{eff} is the effective heat conductivity of the porous medium, which can be defined as:

$$\lambda_{eff} = \varphi \lambda_{liquid} + (1-\varphi)\lambda_{solid} \qquad (17)$$

Discretization of the Equations

First by discretise the thermo poroelastic governing equations by using Greens' theorem [16] to derive equations weak formulations. The weak form of mass, energy, and momentum balance in Eqs. (4), (11), and (14) can be written as below respectively:

$$\int_\Omega w S_s \frac{\partial p}{\partial t} d\Omega + \int_\Omega w^T \alpha \nabla \cdot \frac{\partial \vec{u}}{\partial t} d\Omega + \int_\Omega w \beta \frac{\partial T}{\partial t} - \int_\Omega \nabla w^T \cdot q_H d\Omega + \int_{\Gamma_H^q} w (q_H \cdot n) d\Gamma - \int_\Omega w Q_H d\Omega = 0 \qquad (18)$$

$$\int_{\Gamma_d} wb_m S_s \frac{\partial p}{\partial t} d\Gamma + \int_{\Gamma_d} w\alpha \frac{\partial b_m}{\partial t} d\Gamma + \int_{\Gamma_d} w\beta \frac{\partial T}{\partial t} d\Gamma - \int_{\Gamma_d} \nabla w^T \cdot (b_h q_H) d\Omega + \int_{\Gamma_H^q} wb_h (q_H \cdot n) d\Gamma + \int_{\Gamma_d} wq_H^+ d\Gamma + \int_{\Gamma_d} wq_H^- d\Gamma = 0 \quad (19)$$

$$\int_{\Omega} wc_p \rho \frac{\partial T}{\partial t} d\Omega + \int_{\Omega} wc_p \rho q_H \cdot \nabla T d\Omega - \int_{\Omega} \nabla w^T \cdot (-\lambda \nabla T) d\Omega + \int_{\Gamma_T^q} w(-\lambda \nabla T \cdot n) d\Gamma - \int_{\Omega} w^T Q_T d\Omega = 0 \quad (20)$$

$$\int_{\Gamma_d} wb_m c_p^l \rho^l \frac{\partial T}{\partial t} d\Gamma + \int_{\Gamma_d} wc_p^l \rho^l b_h q_H \cdot \nabla T d\Gamma - \int_{\Gamma_d} \nabla w^T \cdot (-b_m \lambda^l \nabla T) d\Gamma + \int_{\Gamma_T^q} w(-b_m \lambda^l \nabla T \cdot n) d\Gamma + \int_{\Gamma_d} wq_T^+ d\Gamma + \int_{\Gamma_d} q_T^- d\Gamma = 0 \quad (21)$$

$$\int_{\Omega} \nabla^s w^T \cdot (\sigma' - \alpha pI) d\Omega - \int_{\Omega} w^T \cdot \rho g d\Omega - \int_{\Gamma_t} w^T \cdot \vec{\vec{t}} d\Gamma - \int_{\Gamma_d} w^{+T} \cdot \vec{t}_d^+ d\Gamma - \int w^{-T} \cdot \vec{t}_d^- d\Gamma = 0 \quad (22)$$

where, w is the test function; Ω is the model domain; Γ is the domain boundary; t is the traction vector; superscripts +/- refer to the value of the corresponding parameters on opposite sides of the fracture surfaces; respectively, S_s is the specific storage; n is the porosity; q_H is the volumetric Darcy flux; β is the thermal expansion coefficient; Q_H is the fluid sink/source term between the fractures; q_T is the heat flux; cp is the specific heat capacity; b_m and b_h are mechanical and hydraulic fracture apertures; Q_T is the heat sink/source term; α is the thermal expansion coefficient; λ is the thermal conductivity; and *d* refers the fracture plane.

Then the Galerkin method used to spatially discretize the weak forms of Eq. (18) to Eq. (22). The primary variables of the field problem are pressure p, temperature T and displacement vector *u*. All of these variables are approximated by using the interpolation function in finite element space as follow:

$$u = N_u \bar{u} \quad (23) \qquad p = N_p \bar{p} \quad (24) \qquad T = N_T \bar{T} \quad (24)$$

Where: N is the corresponding shape function and $\bar{u}$; $\bar{p}$ and $\bar{T}$ are the nodal unknown values.

3. Results and Discussions

Figure 3 shows the fractures aperture change with stimulation time. As can be seen from the Fig.3, at the first 3 weeks of water injection, the fracture aperture increased at very slow rate. This is due to the fact that at early stage of stimulation, the pressure starts to build up near the injection well and hence fracture aperture starts to enlarge. After the 3 weeks of injection, the fracture aperture starts to grow at much faster rate and covers larger volume. By end of week 12, the stimulation produced a 2.5 fold increase in fracture aperture. In this study, the predicted changes in fracture aperture are in a good agreement with the field data obtained from Soultz geothermal reservoirs [17]. The effect of injected high fluid pressure after 2 weeks and 12 weeks are shown in Fig.4 a, b. After 3 weeks (see Fig.4a) the pressure is quiet high near the injection well. As the injection continuous by the end of 12 weeks (see Fig.4b), the pressure dissipate throughout the entire reservoir region. Figure 5 shows the alteration of permeability values due to stimulation process.

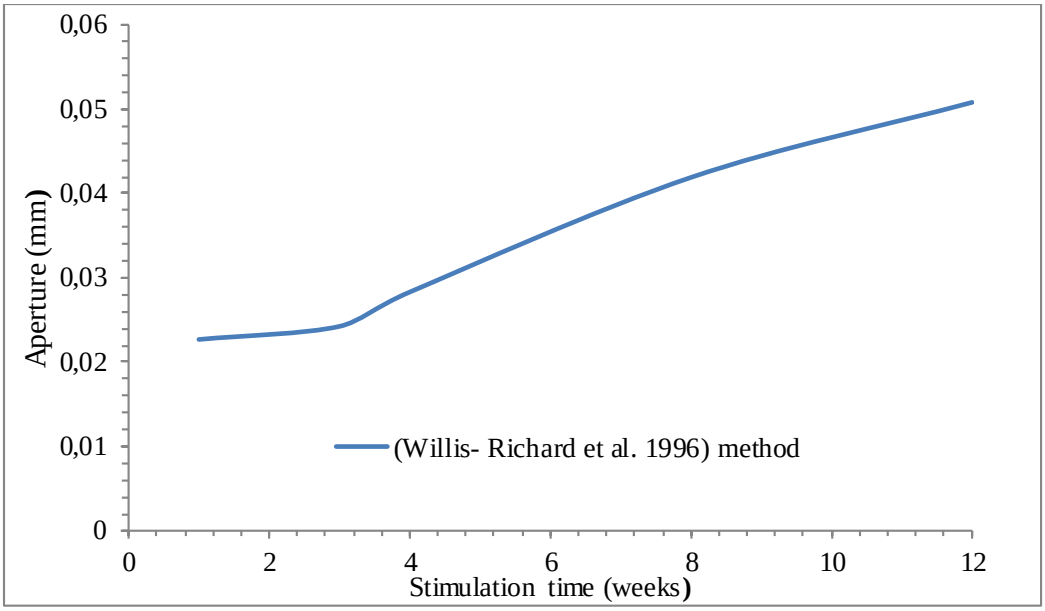

Fig.3. Average increase in fractures aperture due to stimulation process with P_{inj}=42.5MPa, σ_H =91.06MPa, σ_h =49.5MPa, and σ_v =91.78MPa

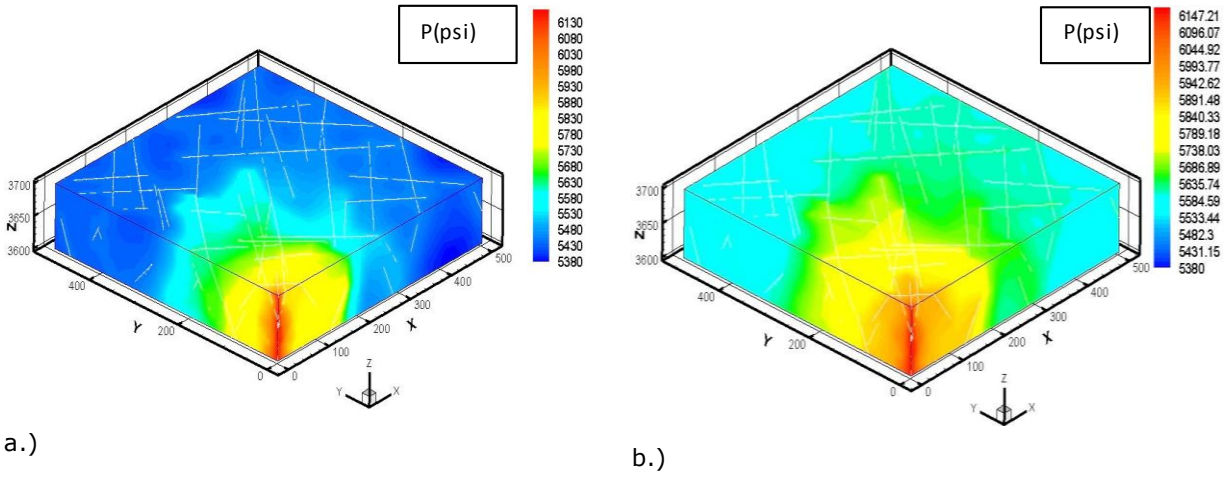

a.)

b.)

Fig.4. Reservoir pore pressure distribution at different stimulation time. Top (a) after 2 weeks and bottom (b) after 10 weeks with P_{inj}=42.5MPa, σ_H =91.06MPa, σ_h =49.5MPa, and σ_v =91.78MPa.

After the reservoir stimulation process is ended and most of the fractures are dilate and their apertures increased, the circulation of cold water over 14 years is simulated to assess the production potential of Soultz reservoir. The reservoir pore pressure distribution after 3 and 14 years of cold water circulation is presented in Fig.7 a, b. As can be seen form these figure (Fig.7a, b) that the reservoir pressure is significantly high around the injection well and with continuous of fluid circulation till 14 years, the pressure reach to a quasi-steady state and the variation of pore pressure remains constant. The change in matrix temperature distributions after 3, 10 and 14 years of cold water circulation are presented in Fig.8. As shown in this figure (see Fig. 8) that the cooling rate is significantly high along the flow path of the cold fluid and this is primarily due to the connected fractures. The significantly high rate of reservoir cooling shows that the temperature draw down is controlled by convective heat transfer as a result of high fluid velocity within the fractures. At the 3 years of cold water injection, the thermal breakthrough is occurred (see Fig.8) and rock temperature starts to drop rapidly and

thus reducing the produced fluid temperature. At 14 years, sweeping of injected cold water covers most of the reservoir region.

Figure 6 shows the components of the effective stresses distribution after 2 weeks and 12 weeks of injection in x-, y- and z- directions respectively. It can be seen from Fig.6 that the pressurization leads to a significant reduction in compressive stress throughout the entire reservoir region.

.

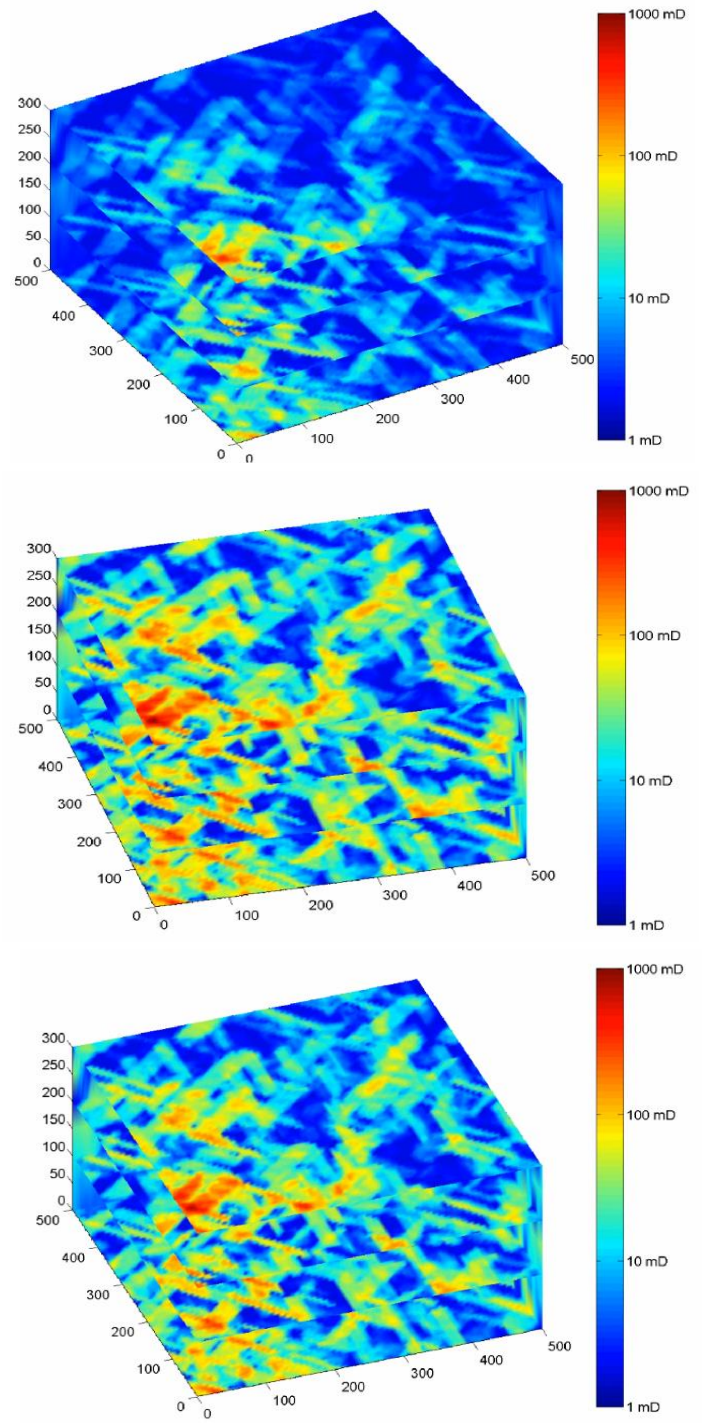

Fig.5. Permeability alteration distribution at different stimulation time. (Top) after 2 hrs, (Middle) after 20 hrs and (Bottom) after 35 hrs of stimulation with P_{inj}=42.5MPa, σ_H =91.06MPa, σ_h =49.5MPa, and σ_v =91.78MPa.

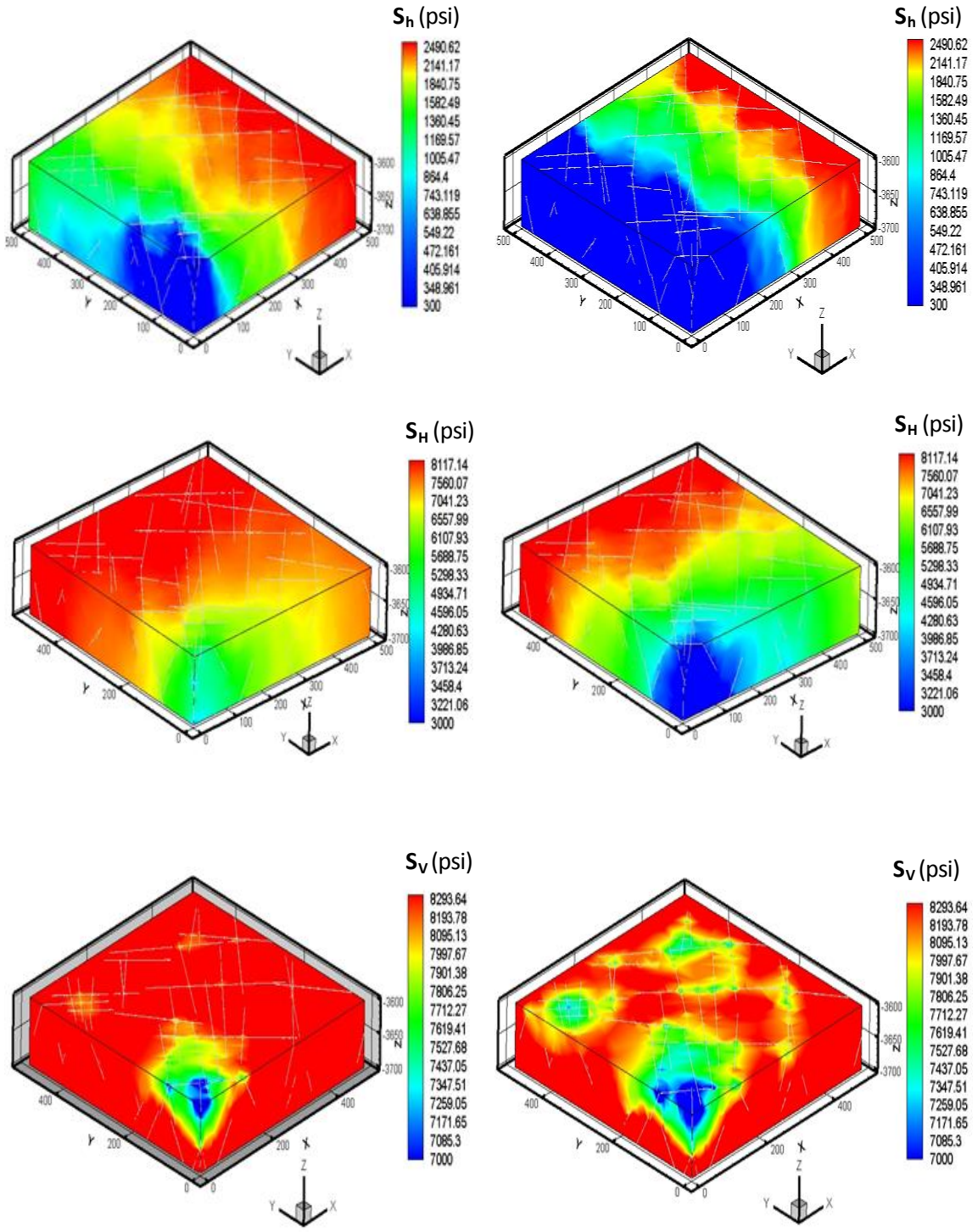

Fig.6. x-, y- and z- components of effective stresses. Top (x-stresses), middle (y-stresses) and bottom (z-stresses) after 10 weeks of stimulation with P_{init}=34.5MPa, P_{inj}=42.5MPa, σ_H =91.06MPa, σ_h =49.5MPa, and σ_v =91.78MPa.

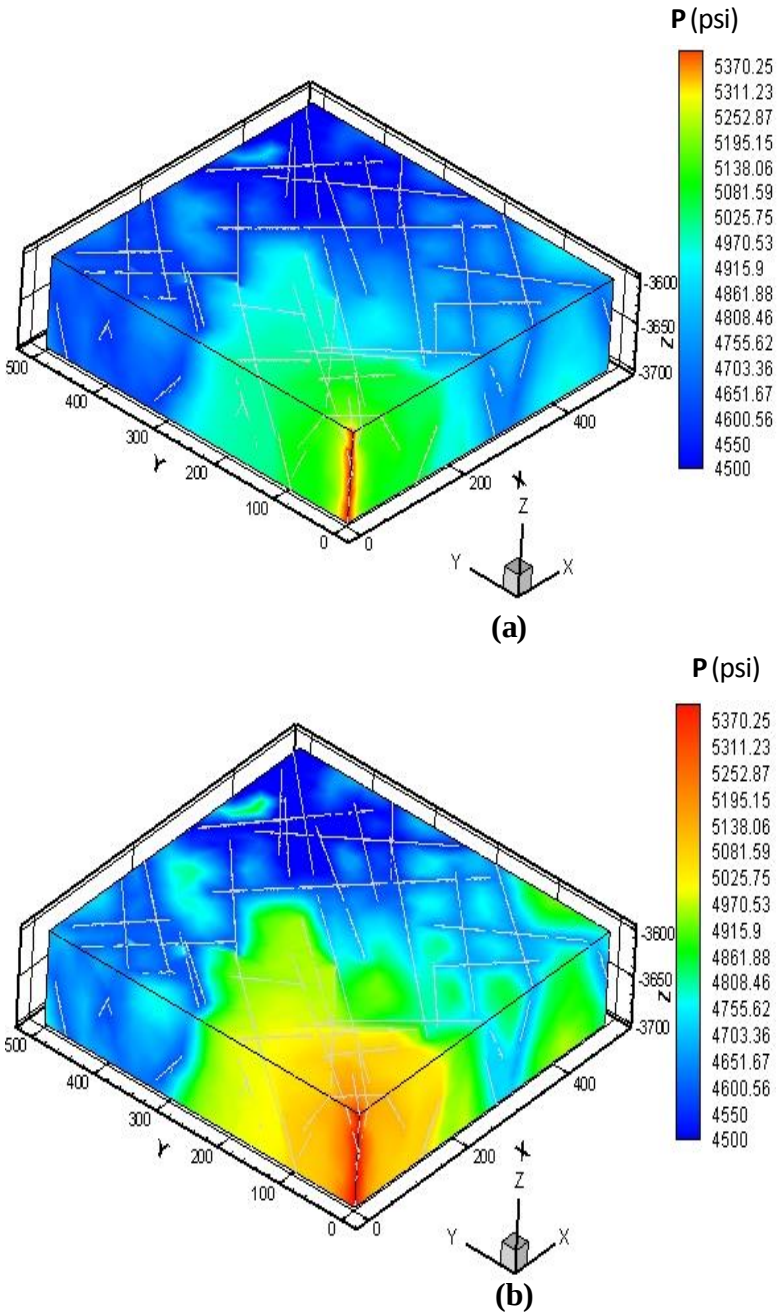

Fig.7. Reservoir pore pressure distribution at different simulation time. Top (a) after 3 years and bottom (b) after 14 years with P_{init}=34.5MPa, P_{inj}=37.5MPa, P_{prod}=31.5MPa σ_H =91.06MPa, σ_h =49.5MPa, and σ_v =91.78MPa.

The x-, y- and z- components of effective stresses distribution after 3 years of cold water injection with and without the effect of thermal stresses are presented in Fig.9. The poroelastic results for effective stresses are presented in Fig.9 (left). The figure shows that the cooled zones around the fractures and near injection well are mostly compressive and become more compressive away from the injection well. In Fig.9 (right) the effect of thermal stresses is significant during the circulation period. As shown in Fig.9 (right) that the thermal stresses due to cooling of rock matrix causes rock contraction that leads to inducing of tensile stress. In addition, thermal contraction could cause tensile fractures throughout the formation. In Fig.9, it is clear that thermal stress produces less compressive stress.

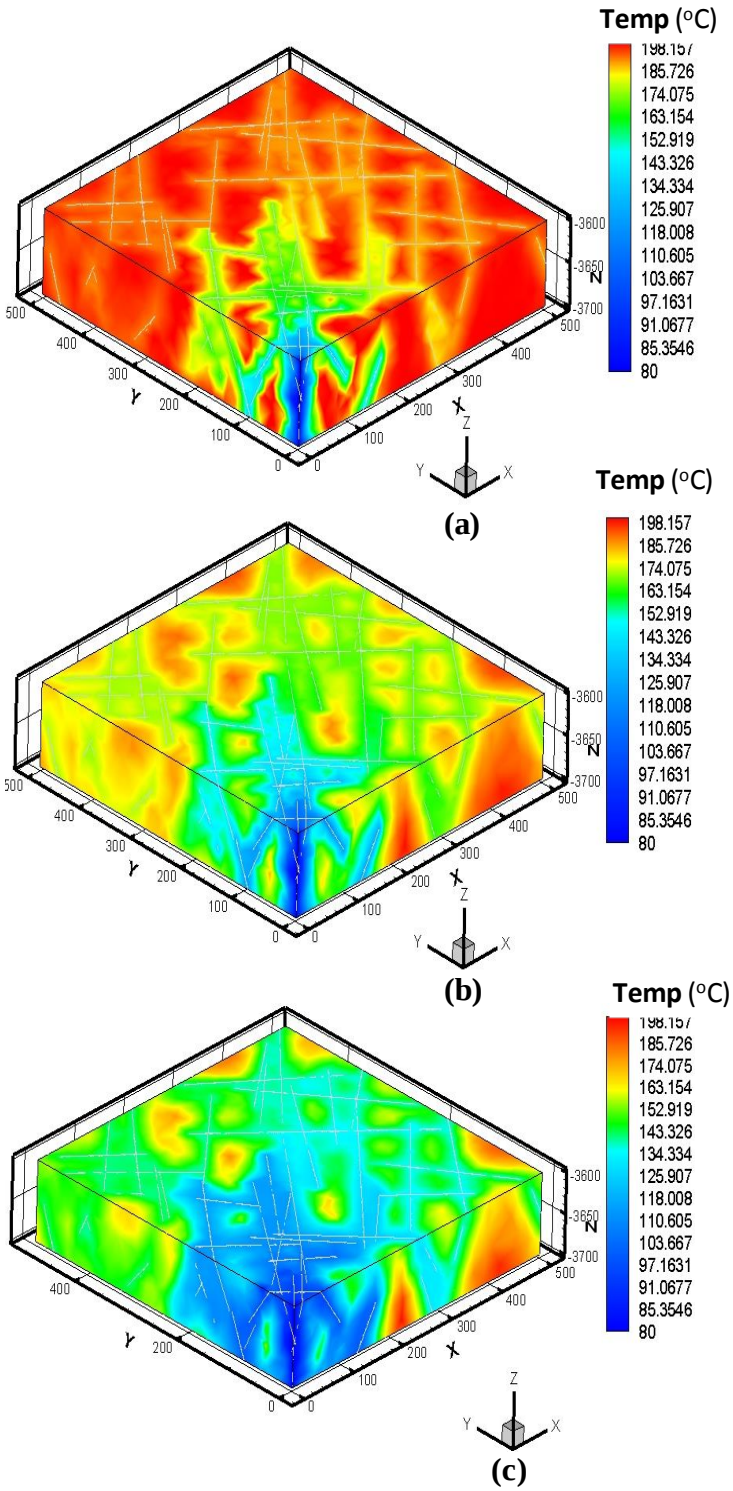

Fig. 8. Reservoir rock temperature distribution at different simulation time. Top (a) after 3 years and middle (b) after 10 years and bottom (c) after 14 years with P_{init}=34.5MPa, P_{inj}=37.5MPa, P_{prod}=31.5MPa σ_H =91.06MPa, σ_h =49.5MPa, σ_v =91.78MPa and T_{inj}=80°C.

Furthermore, thermal stress causes the produced fluid temperature during the production period to decrease (see Fig.10), in particular once the breakthrough of the circulating fluid takes place. This is due to the fact that thermal stress helps to increase the fracture aperture

which in turn increases the injectivity of the well and leads to creation of flow channeling between the injection and production wells.

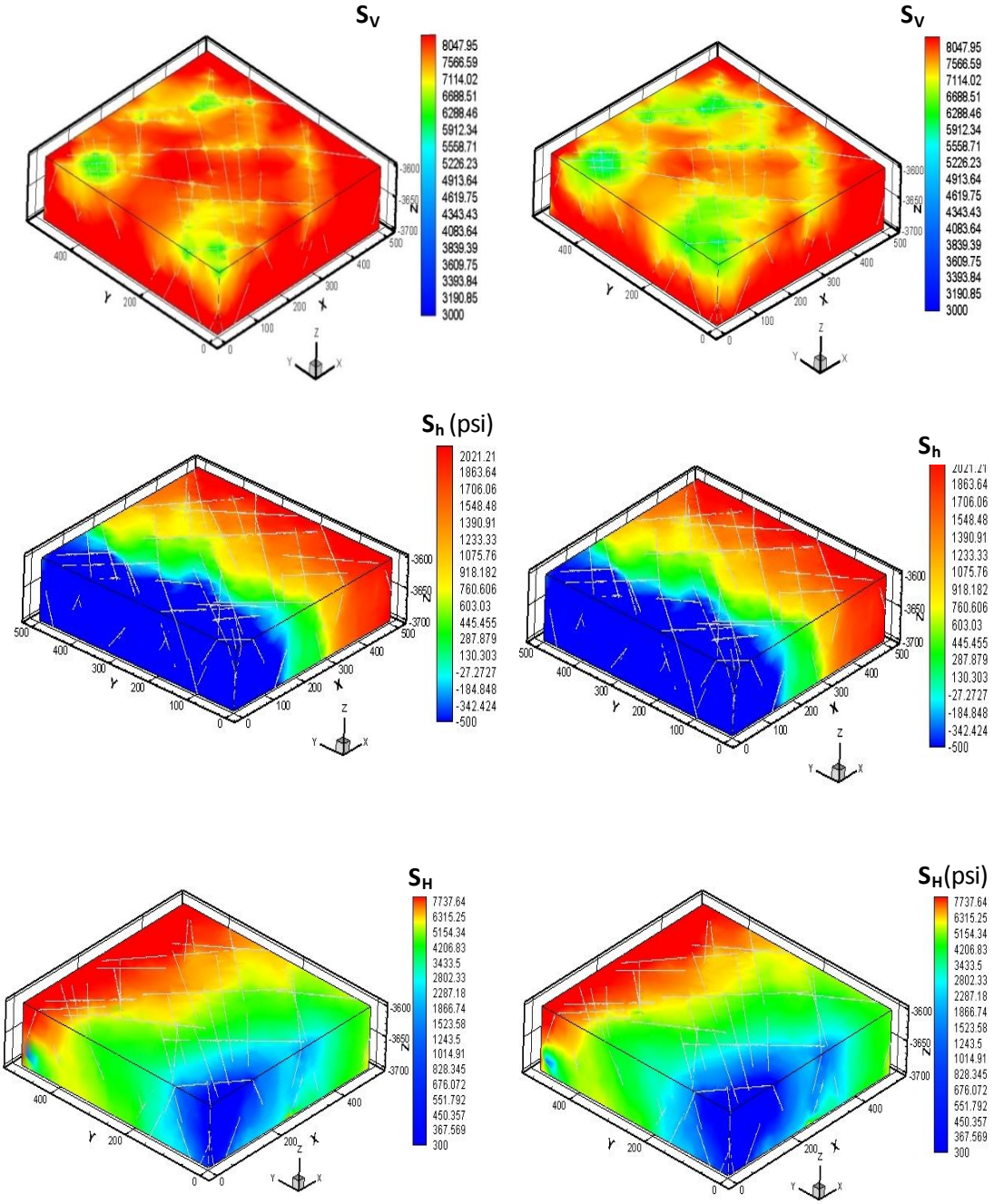

.

Fig. 9. z-, x- and y- components of effective stresses. Top (z-stresses), middle (x-stresses) and (y-stresses) after 3 years of cold water circulation without (left) and with (right) consideration of thermal stresses with P_{init}=34.5MPa, P_{inj}=42.5MPa, σ_H =91.06MPa, σ_h =49.5MPa, σ_v =91.78MPa and T_{inj}=80°C.

In this study, the difference between the produced fluid temperature with and without thermal stress effect at 14 years of fluid circulation is 7 °C. These interpretations of the effect of thermal stress on produced fluid temperature are in a good agreement with that obtained from a typical geothermal reservoir study presented by Hicks *et al.* [18]. As mentioned above the produced fluid temperature remained unchanged for about first three years of cold water circulation. Then the temperature starts to decline until 14 years. This is attributed to the effect of reservoir pressurization which opens up fluid paths in parts of the reservoir which was not connected previously. With the pass of time, a large number of fractures are contributing to the fluid flow which increases heat transfer from rock to fluid thus cooling the reservoir faster.

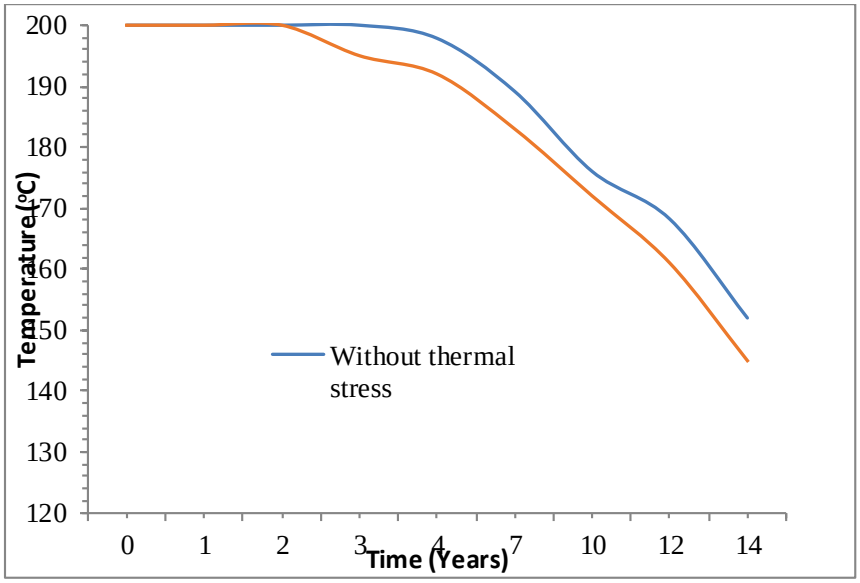

Fig.10. Produced fluid temperature with time with and without consideration the effect of thermal stresses with P_{init}=34.5MPa, P_{inj}=37.5MPa, P_{prod}=31.5MPa σ_H =91.06MPa, σ_h =49.5MPa, σ_v =91.78MPa and T_{inj}=80°C.

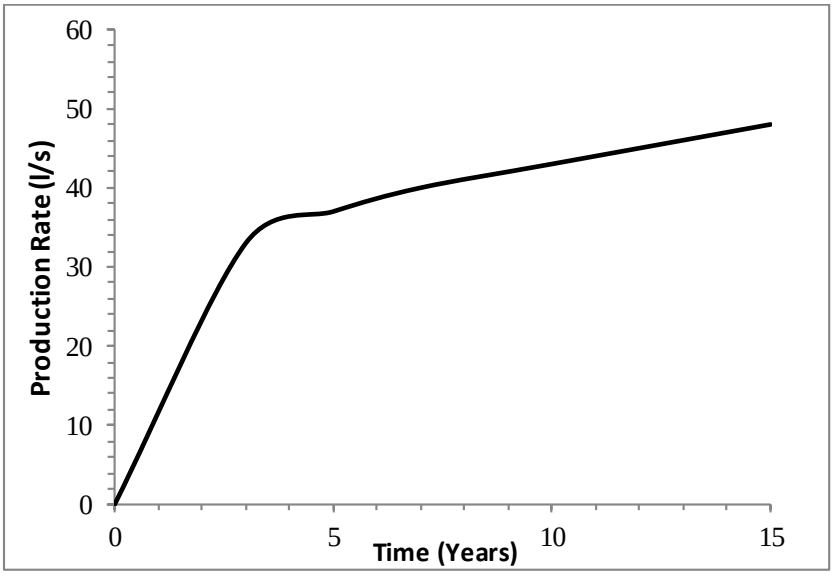

Fig.11. Reservoir producing flow rate during 14 years of cold water circulation with P_{init}=34.5MPa, P_{inj}=37.5MPa, P_{prod}=31.5MPa σ_H =91.06MPa, σ_h =49.5MPa, σ_v =91.78MPa and T_{inj}=80°C

The production rate versus simulation time for the Soultz geothermal reservoir is presented in Fig.11. This figure shows that the production rate sharply increased at the first three years

of cold fluid circulation then increasing rate becomes slower. This is due to the fact that the pressure impedance between the injection and production well is kept constant (6MPa) and as expected after a certain period of circulation, the production rate become stable due to stabilization of pressure within the reservoir.

4. Conclusion

Geothermal energy from hydrothermal is an option to cover part of the future electricity demand to guarantee energy security. The thermal stress force and pressure solution can result in a significant change in the fracture aperture and permeability. Thus, the importance of these changes may give rise to a significant coupling between thermal stress, mechanical and hydrological processes. Understanding of these couplings with the simulation results are extremely valuable for monitoring the geothermal reservoir and determining the amount of heat that produced with time.

This study aims at understanding the long term behavior of geothermal reservoir by interpreting the coupled processes. In this study, the improvement in reservoir permeability by fluid pressurization is investigated by a shear displacement model in a poro-thermo-elastic framework. The poro-thermo-elastic model was used to assess the potential of the Soultz geothermal reservoir in France. The obtained results are in good agreement with the experience of current EGS (Enhanced Geothermal Systems) trials around the world, such as in Rosemanowes, Soultz and Habanero reservoirs. The results of cold fluid circulation show that tensile normal stresses, due to the circulation of cold fluid, tend to increase fracture apertures within the zone of cooling. This increase in aperture, and hence the permeability, is evident predominantly near the wellbore region in the early circulation period. Over longer periods, a significant part of the reservoir, through which circulation is well established, is subjected to larger thermal stresses. These thermal stresses consequently increase the permeability of the major interconnected fractures, which in turn increase the flow rate at fixed pressure impedance. It is noteworthy that during the fluid injection, especially over longer term, appropriate monitoring and mitigation strategies have to be utilized to monitor earthquakes.

References

[1] Bundschuh J. (2010). Introduction to the numerical modeling of groundwater and geothermal systems: fundamentals of mass, energy and solute transport in poroelastic rocks. CRC Press.

[2] Sanyal SK and Butler SJ. (2004). National assessment of US enhanced geothermal resource base–a perspective. Geothermal Resources Council Transactions, 28.

[3] De Boer RB, Nagtegaal PJ C and Duyvis EM. Pressure solution experiments on quartz sand. Geochimica et Cosmochimica Acta, 1997; 41(2), 257IN1261-260IN4264.

[4] Yasuhara H, Elsworth D and Polak A. Evolution of permeability in a natural fracture: Significant role of pressure solution. Journal of Geophysical Research: Solid Earth, 2004; 109 (B3).

[5] Lowell RP and Germanovich N. (1994). On the temporal evolution of high-temperature hydrothermal systems at ocean ridge crests. Journal of Geophysical Research: Solid Earth, 1994; 99(B1), 565-575.

[6] Kumar GS and Ghassemi A. Numerical modeling of non-isothermal quartz dissolution/precipitation in a coupled fracture–matrix system. Geothermics, 2005; 34(4), 411-439.

[7] Taron J, Elsworth D and Min KB. Numerical simulation of thermal-hydrologic-mechanical-chemical processes in deformable, fractured porous media. International Journal of Rock Mechanics and Mining Sciences, 2009; 46(5), 842-854.

[8] Koh J, Roshan, H and Rahman SS. A numerical study on the long term thermo-poroelastic effcts of cold water injection into naturally fractured geothermal reservoirs. Computers and Geotechnics, 2011; 38(5), 669-682.

[9] Ghassemi A, and Kumar GS. Changes in fracture aperture and fluid pressure due to thermal stress and silica dissolution/precipitation induced by heat extraction from subsurface rocks. Geothermics, 2007; 36(2), 115-140.

[10] McDermot, C, and Kolditz O. Geomechanical model for fracture deformation under hydraulic, mechanical and thermal loads. Hydrogeology Journal, 2006; 14(4), 485-498.
[11] O'Sullivan MJ, Pruess K, and Lippmann MJ. (2001). State of the art of geothermal reservoir simulation. Geothermics, 2001; 30(4), 395-429.
[12] Shaik AR, Rahman SS, Tran NH, Tran T. (2011). Numerical simulation of fluid-rock coupling heat transfer in naturally fractured geothermal system. Applied thermal engineering, 2011; 31(10): 1600-1606.
[13] Willis-Richards J, Watanabe K, and Takahashi H. Progress toward a stochastic rock mechanics model of engineered geothermal systems. Journal of Geophysical Research: Solid Earth (1978–2012), 1996; 101(B8), 17481-17496.
[14] Doonechaly NG, Rahman SS. 3D hybrid tectono-stochastic modeling of naturally fractured reservoir: Application of finite element method and stochastic simulation technique. Tectonophysics, 2012; 541: 43-56.
[15] Watanabe N, Wang W, McDermott CI, Taniguchi T and Kolditz O. Uncertainty analysis of thermo-hydro-mechanical coupled processes in heterogeneous porous media. Computational Mechanics, 2010; 45(4): 263-280.
[16] Bathe KJ. Finite element procedures. Prentice-Hall, Englewood Cliffs, 1996, New Jersey
[17] Evans KF, Genter A, Sausse J. (2005). Permeability creation and damage due to massive fluid injections into granite at 3.5 km at Soultz: 1. Borehole observations. Journal of Geophysical Research: Solid Earth, 2005; 110(B4).
[18] Hicks T, Pine R, Willis-Richards J, Xu S, Jupe A, and Rodrigues N. (1996). A hydro-thermo-mechanical numerical model for HDR geothermal reservoir evaluation. Paper presented at the International journal of rock mechanics and mining sciences & geomechanics abstracts.
[19] Shaik AR, Rahman SS, Tran NH, and Tran T. Numerical simulation of fluid-rock coupling heat transfer in naturally fractured geothermal system. Applied thermal engineering, 2011; 31(10), 1600-1606.

To whom correspondence should be addressed: Dr. Reda Abdel Azim, American University of Ras Al Khaimah, United Arab of Emirates, Ras Al Khaimah, Email: reda.abdelazim@aurak.ac.ae